

# DESIGN OF A PROOF-OF-PRINCIPLE EXPERIMENT TOWARD THE GENERATION OF COHERENT OPTICAL RADIATION USING A 4-MeV ELECTRON BEAM\*

Y.-E Sun, P. Piot, Fermi National Accelerator Laboratory, Batavia, IL 60510, USA  
 D. Mihalcea, H. Panuganti, P. Piot  
 Department of Physics, Northern Illinois University, DeKalb, IL 60115, USA  
 W.S. Graves, Massachusetts Institute of Technology, Cambridge, MA 02139, USA

## Abstract

Transverse-to-longitudinal phase-space-exchange techniques have opened new possibilities towards shaping the temporal distribution of electron beams. Sub-ps bunch trains have been experimentally realized at the A0 photoinjector at Fermilab. Recently, the combination of such emittance-exchange methods with nanocathode arrays was suggested as the backbone of compact coherent short-wavelength sources. In this paper, we discuss a possible proof-of-principle experiment to produce coherent optical transition radiation using a  $\sim 4$  MeV electron bunch. The optically-modulated bunch is produced from a structured cathode combined with a transverse-to-longitudinal phase space exchanger.

## INTRODUCTION

It is well known that radiation produced by a bunch of charged particles is greatly enhanced when observed at wavelengths of the order or shorter than the bunch length. In general, the spectral angular fluence emitted by a bunch of  $N \gg 1$  electrons from any electromagnetic process is related to the single-electron spectral fluence,  $\frac{d^2W}{d\omega d\Omega} \Big|_1$ , via

$$\frac{d^2W}{d\omega d\Omega} \Big|_N \simeq \frac{d^2W}{d\Omega d\omega} \Big|_1 [N + N^2 |S(\omega)|^2]$$

where  $\omega \equiv 2\pi f$  ( $f$  is the frequency) and  $S(\omega)$ , the bunch form factor (BFF), is the intensity-normalized Fourier transform of the normalized charge distribution  $S(t)$  [1]. The former equation assumes the bunch can be approximated as a line charge distribution. Considering a series of  $N_b$  identical bunches with normalized distribution  $\Lambda(t)$  we have  $S(t) = N_b^{-1} \sum_{n=1}^{N_b} \Lambda(t + nT)$  (where  $T$  is the period between the bunches) giving  $|S(\omega)|^2 = \xi |\Lambda(\omega)|^2$  where  $\Lambda(\omega)$  is the Fourier transform of  $\Lambda(t)$  and the intra-bunch coherence factor  $\xi \equiv N_b^{-2} \sin^2(\omega N_b T/2) / [\sin^2(\omega T/2)]$  describes the enhancement of radiation emission at the resonant frequencies  $\omega_n = 2\pi n/T$ .

Therefore, coherent optical radiation can be produced by a train of electron bunches with sub-micron separation. The

recent experimental demonstration of sub-picosecond electron bunch train generation using an emittance exchange (EEX) technique [2] and its use to produce narrow-band Terahertz transition radiation [3] has open new possibilities.

Recently, it was proposed to adapt this method to generate vacuum-ultraviolet and possibly x-ray coherent radiation using inverse Compton scattering of a pre-bunched beam [4]. Downscaling the pre-bunching wavelength by emittance-exchanging a transversely-segmented beam obtained via interception of the beam with a multi-slit mask is challenging. Instead, Ref. [4] proposes to produce the needed transversely-segmented beam using a patterned cathode such as a field emitter array (FEA). Experimentally validating such a concept is of importance: as the bunch spacing becomes shorter, deleterious effects (such as, e.g., thick-lens effects associated to the deflecting cavity) are more prominent and can significantly impact the EEX process. Therefore, we are exploring such an experiment using the EEX beamline readily available at Fermilab in combination with a FEA cathode to be installed in the available L-band rf gun. This paper describes our plans and provides some numerical simulations supporting the possible generation of optically-modulated beams.

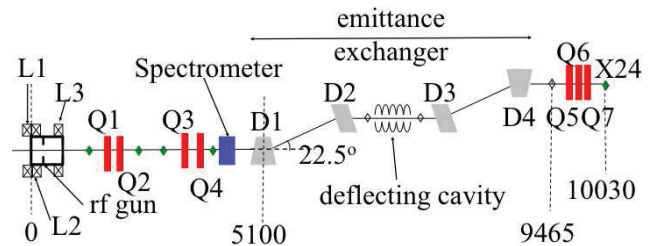


Figure 1: Schematic drawing of the HBESL beamline. A set of four quadrupoles (Q1-Q4) are used to tune the beam transverse phase space parameters at the entrance of the EEX beamline, which includes the four dipole magnets (D1-D4) and the deflecting cavity.

\*Work supported by DOE under contract No. DE-AC02-07CH11359 with the Fermi Research Alliance, LLC and by DARPA under grant No. N66001-11-1-4192 with MIT.

## HBESL BEAMLINE

The High Brightness Electron Source Lab. (HBESL) at Fermilab is a newly-reconfigured beamline from the previous A0 photoinjector [5] which operated from 1998 to 2011. In brief, electron bunches are nominally photoemitted from a cesium telluride ( $\text{Cs}_2\text{Te}$ ) photocathode located on the back plate of a 1+1/2 cell radio-frequency (rf) cavity operating at 1.3 GHz (the “rf gun”). The rf gun is surrounded by three solenoidal lenses that control the beam’s transverse size and emittance. The beam then propagates through a beamline that includes quadrupole and steering dipole magnets, and diagnostics stations. Under nominal operation the beam is bent vertically and dumped. The beam can also be sent to the original EEX beamline which was utilized at A0 for the demonstration of emittance exchange [6]. The EEX assembly is composed of a 3.9-GHz deflecting rf cavity, operating on the  $\text{TM}_{110}$  like  $\pi$ -mode, located between two magnetic doglegs, each comprising two dipole magnets; see Fig. 1.

The facility incorporates two photocathode drive laser systems. The nominal A0 photoinjector laser which consists of a frequency-quadrupled Neodymium-doped yttrium lithium fluoride (Nd:YLF) laser [7] producing laser pulses with duration  $\sim 3$  ps and a Titanium-Sapphire (Ti:Sp) oscillator and regenerative amplifier were installed [8]. The Ti:Sp system incorporates an acousto-optic programmable dispersive filter system to control the laser shape [9, 10] and generates 3.5-mJ infrared (IR) pulses ( $\lambda = 800$  nm) with duration of  $\sim 100$  fs (rms) that are nominally frequency-trippled to photoemit electrons from the  $\text{Cs}_2\text{Te}$  photocathode.

## NUMERICAL SIMULATIONS

### Field-emission Source

The particle distribution file is generated such that it accounts for the field-emission process and for the geometry of the emitting surface. To determine the radial distribution of the charge, the emitting surface is divided into a certain number of concentric zones (centered on the tip) and the external field is averaged for each zone. The radial particle density in a certain zone is taken proportional with the current density of the zone determined from the average external field through the Fowler-Nordheim equation [11]. The number of zones is limited by the density of points in the external field map. We require that within each zone there is at least one point in the external field map. To determine the longitudinal charge distribution the time dependent electric field at the emitting surface should be known. At this time the external field is assumed static so the longitudinal charge distribution is constant. Still, the front and the end shapes of the bunch are consistent with the emitting surface. The particle distribution is generated underneath the emitting surface and is advanced due to a small initial longitudinal momentum. These simulations of field emission are carried with a modified version

of IMPACT-T [12].

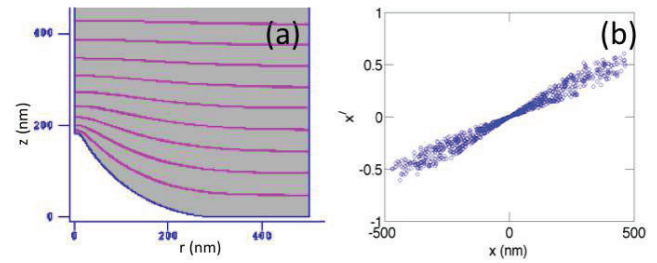


Figure 2: Geometry for the field-emitter (a) and simulated transverse-trace-space ( $x, x' \equiv p_x/p_x$ ) macroparticle distribution 500-nm downstream of the tip (b).

Given the beam phase-space macroparticle distribution  $F(\mathbf{x}, \mathbf{p})$  obtained few 100’s nm away from the tip, a FEA is simulated numerically and its distribution was obtained by copmabing the single-emitted distribution following

$$\Phi(x, y, z, \mathbf{p}) = \sum_{i=-m}^m \sum_{j=-n}^n F(x + i\delta x, y + j\delta y, z, \mathbf{p}),$$

where  $\delta x$  (resp.  $\delta y$ ) is the horizontal (resp. vertical) pitch,  $\mathbf{x} \equiv (x, y, z)$  are the usual cartesian coordinates and  $\mathbf{p} \equiv (p_x, p_y, p_z)$  is the momentum. In the following we only considered arrays composed of an odd number of field-emitter cathodes with its central beamlet centered on the origin.

The single-tip geometry considered throughout this paper is schematized in Fig. 2 with the associated phase-space macroparticle distribution obtained 500 nm downstream of the tip. Other geometries are also under considerations. The electrostatic field map was simulated using the POISSON/SUPERFISH software suite [13]. For the beam dynamics simulations, the tip was taken to produce a 100- $\mu\text{A}$  average current during a 100-fs duration (corresponding to the Ti:Sp laser system parameters) resulting in the emission of  $\sim 200$  electrons per tip. The beam dynamics throughout the rf gun is performed with IMPACT-T and space charge effects are generally found to be negligible.

### Single-particle Dynamics

The beam dynamics simulation of the entire setup were first conducted with a combination of IMPACT-T and ELEGANT [14]. The initial beam distribution is generated from a nano-tip (spherical radius 22 nm) using the PIC code Impact-T and ELEGANT. IMPACT-T is used to track the distribution generated by the FEA throughout the beamline up to the entrance of the first quadrupole magnet (Q1 at  $z \simeq 2$  m from the cathode; see Fig. 1) while ELEGANT enable the optimization of the beam dynamics from quadrupole magnet Q1 to the EEX exit.

Iterative IMPACT-T and ELEGANT simulations were carried to select optimum operating parameters (gun phase, solenoid peak field, and quadrupole-magnet strengths) that

produce the best final modulation. Given the fact that the initial beam distribution is no cylindrical symmetric (we use a square  $7 \times 7$  FEA array) and to avoid complication resulting from  $x - y$  coupling, we rotated the initial FEA distribution to compensate for the Larmor rotation that occurs during transport through the solenoid. The cavity was first model by its thin-lens transfer matrix and then using a thick-lens matrix

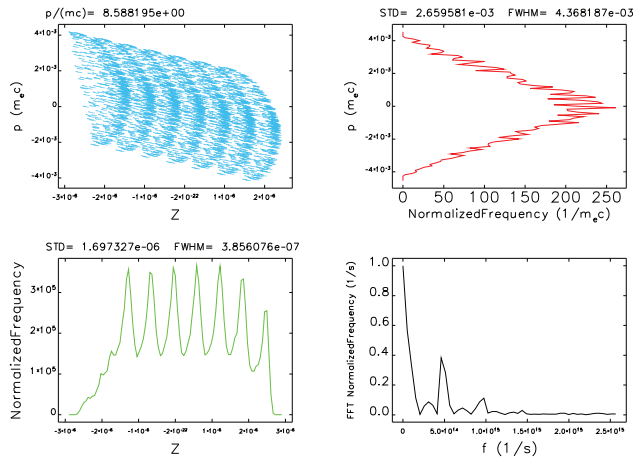


Figure 3: Longitudinal phase space (top left) downstream of the EEX beamline with corresponding energy (top right) and temporal (bottom left) profiles and associated bunch form factor (bottom right). These simulations are carried for an idealized thin-lens model of the deflecting cavity.

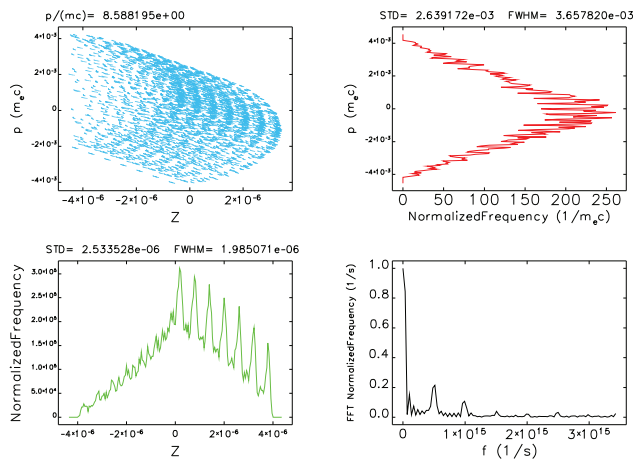


Figure 4: Longitudinal phase space (top left) downstream of the EEX beamline with corresponding energy (top right) and temporal (bottom left) profiles and associated bunch form factor (bottom right). These simulations are carried for a realistic thick-lens model of the deflecting cavity.

The optimization capabilities of ELEGANT were used to find the Q1-Q4 quadrupole strengths that results in the final longitudinal phase space associated to one beamlet to be up-right. We follow the prescription detailed in Ref [15].

The resulting final longitudinal phase spaces obtained for an ideal (thin-lens) and realistic model of the deflecting cavity are respectively shown in Fig. 3 and Fig. 4. The idealized case is worth investigating as it could in principle be practically implemented by adding a single-cell accelerating cavity downstream of the deflecting cavity [16]. The two cases show bunching at the same wavelength ( $\sim 700 \mu\text{m}$ ) with respective bunching factor of 0.4 (idealized) and 0.2 (realistic) consistent with the production of coherent optical radiation. The observed modulation wavelength corresponds to a compression factor of 2 compared to the initial FEA pitch ( $1.5 \mu\text{m}$ ).

### Preliminary Multi-particle Dynamics

Start-to-end multiparticle simulations were also carried using GENERAL PARTICLE TRACER (GPT) [17]. The starting macroparticle distribution at the cathode location was the one generated with IMPACT-T. The deflecting mode cavity was simulated using a 3-D electromagnetic field map obtained from HFSS [18]. The solenoids and quadrupole magnets were empirically optimized using some of the results obtained from ELEGANT simulations to achieve up-right beamlets in the final longitudinal phase space.

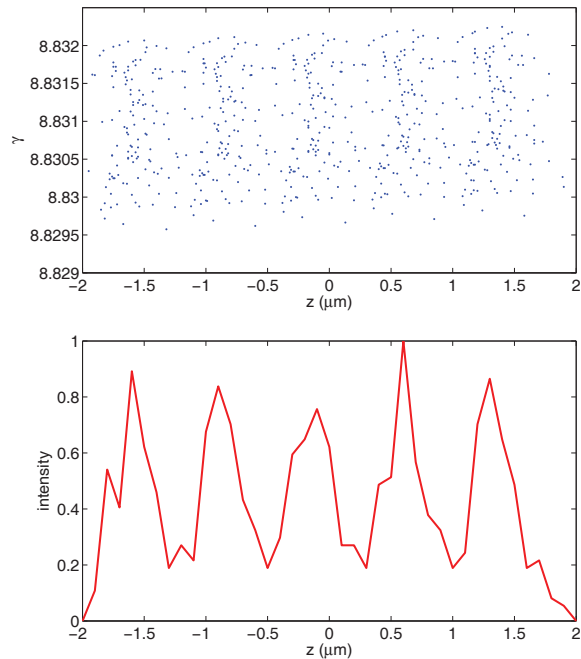


Figure 5: Longitudinal phase space downstream of the EEX beamline (top) and corresponding temporal profile (bottom) simulated with the GPT program.

As depicted in Fig. 5, a modulation in the infrared regime ( $\approx 700 \text{ nm}$ ) could be obtained. The longitudinal phase space displays some notable difference compared to the phase spaces presented in the previous sections. These discrepancies are not understood and still being investigated.

## EXPERIMENT PLANS AND STATUS

In order to quantify the generation of modulated bunches in the infrared and optical regimes, we plan on detecting backward transition radiation emitted as the beam hits an aluminum target located downstream of the EEX beamline (at X24 in Fig. 1). At our energies ( $\gamma \simeq 9$ ), the angular distribution of transition radiation is very broad [see Fig. 6 (a)] and only 30% of the total radiated energy shines out of a 2''-diameter optical vacuum window. Informations on the modulation wavelength and amplitude can then be obtained from a spectral analysis of the radiation [19]. In a

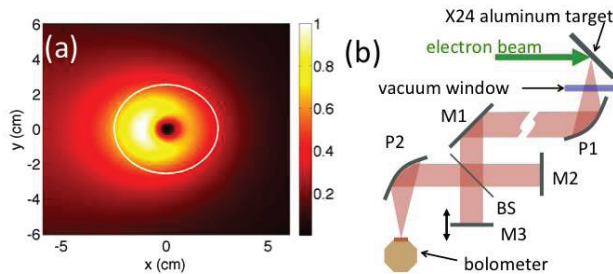


Figure 6: Optical transition radiation spatial distribution produced by a 4.5 MeV electron at the vacuum window exit (a) and initial experimental setup to detect infrared backward coherent transition radiation (b). The white circle in (a) delineates the aperture imposed by a 2''-diameter optical vacuum window.

first phase, we plan on modifying the setup used in Ref. [2] and schematized in Fig. 6 (b). In this configuration, the radiation shining out of an optical vacuum window is collected and collimated by a large-aperture off-axis parabolic mirror (P1) before being sent to a Michelson autocorrelator (composed of planar mirrors M1, M2, beam splitter BS, and parabolic off-axis mirror P2) [20]. The autocorrelated radiation is detected by a highly-sensitive Helium-cooled bolometer. Such a setup should enable the detection of infrared modulations. In a second phase, the setup will be modified to include an intensified CCD camera capable of detecting low-intensity optical radiation. The electron beam's transverse density will be imaged on the camera CCD chip and enhancement of the radiation intensity will be a signature of optical modulation. In addition, we will also attempt to locate this camera downstream of a diffraction grating to directly measure the spectrum and see the enhanced wavelengths.

Presently, the HBESL facility is being commissioned and measurement of optical transition radiation at low energy will be attempted in the upcoming weeks to assess whether the available intensified camera can be used to detect and possibly measure the spectrum of the optical transition radiation emitted from a low-energy beam. In parallel the EEX beamline is being reassembled and modified to accommodate the experimental plans described in this paper.

## SUMMARY

Preliminary simulations indicate that an extension of the beamlet-generation experiment presented in Ref. [2] from the THz to optical regime appears to be feasible. This two-orders of magnitude improvement in modulation wavelength will be carried with a  $\sim 4$  MeV beam (compared to 14 MeV in the THz-generation experiment). Experimentally realizing such a downscaling in modulation wavelength, obtained by combining the EEX method with a FEA cathode, is an important step toward the design of a compact ultraviolet coherent light source based on inverse Compton scattering.

## ACKNOWLEDGMENTS

We are thankful to Michael Swanwick (MIT) for providing the geometry of a possible field-emitter used in our simulations and Timergali Khabibouline (Fermilab) for HFSS simulations of the 3.9-GHz deflecting mode cavity.

## REFERENCES

- [1] J. S. Nodvick and D. S. Saxon, *Phys. Rev.* **96**, 180 (1954).
- [2] Y.-E. Sun, *et al.*, *Phys. Rev. Lett.* **105**, 234801 (2010).
- [3] P. Piot, *et al.*, *App. Phys. Lett.* **98**, 261501 (2011).
- [4] W. S. Graves, *et al.*, *Phys. Rev. Lett.* **108**, 264904 (2012).
- [5] J.-P. Carneiro, *et al.*, *Phys. Rev. ST Accel. Beams* **8**, 040101 (2005).
- [6] J. Ruan, *et al.*, *Phys. Rev. Lett.* **106**, 244801 (2011).
- [7] J. Li, R. Tikhoplav, A. Melissinos, *Nucl. Instrum. Meth. A.* **564**, 57 (2006).
- [8] T. J. Maxwell, J. Ruan, P. Piot, and A. H. Lumpkin, arXiv:1203.1657v1 (2011).
- [9] P. Tournois, *Opt. Commun.* **140**, 245 (1997).
- [10] Dazzler pulse shaper system from Fastlite, France.
- [11] R. H. Fowler and L. Nordheim, *Proc. R. Soc. London Ser. A* **119**, 173 (1928).
- [12] J. Qiang, R. Ryne, S. Habib, and V. Decyk, *J. Comp. Phys.* **163**, 434 (2000).
- [13] J.H. Billen and L.M. Young, in *Proceedings of the 1993 Particle Accelerator Conference*, Washington, DC (IEEE, Piscataway, NJ, 1993), p. 790.
- [14] M. Borland, "Elegant: A Flexible SDDS-Compliant Code for Accelerator Simulation," *Advanced Photon Source, Light Source Note LS-287*, September 2000.
- [15] P. Piot, W. S. Graves, in preparation (2012).
- [16] A. A. Zholents, *et al.*, ANL/APS/LS-327, May 2011.
- [17] Information on the GENERAL PARTICLE TRACER program can be found at <http://www.pulsar.nl/gpt/>.
- [18] The High Frequency Structure Simulator (HFSS) is a commercial software from Ansys corporation.
- [19] C. Sears, *et al.*, *Phys. Rev. ST Accel. Beams* **11**, 061301 (2008).
- [20] D. Mihalcea, *et al.*, *Phys. Rev. ST Accel. Beams* **9**, 082801 (2006).